

Dynamic Bridge Substructure Condition Assessment with Hilbert Huang Transform with Simulated Flood and Earthquake Damage for Structural Health/Security Monitoring

Ray Ruichong Zhang
Division of Engineering
Colorado School of Mines
Golden, CO 80401
Rzhang@mines.edu

Larry D. Olson, P.E.
Olson Engineering, Inc.
5191 Ward Road, Suite 1
Wheat Ridge, CO 80033
Ph – 303-423-1212
Fx – 303-423-6071
ldolson@olsonengineering.com

word count = 3804
7 figures at 250 words each = 1750
total word count = 5554

Abstract

This study involved modal vibration tests combined with the Hilbert-Huang Transform (HHT) method to analyze previous recordings of controlled field vibration tests of one concrete pile substructure of the Trinity River Relief Bridge No. 4 in Texas in its intact, minor- and severe-damage states. Piles were excavated and broken to simulate flood and earthquake damage to a bridge substructure. The HHT algorithm is unique in that it reveals the quantitative difference in instantaneous frequency of sound and damaged structures, consistent with the damage states and with what a simple structural model predicts. This approach differs from traditional modal vibration analyses in that a short-lived shift downward in resonant frequency can be seen in the HHT from a damaged member, while this shift is often lost due to the averaging effect of a modal vibration analysis. Accordingly, an HHT-based structural health monitoring procedure is discussed herein

INTRODUCTION

Identification of certain vibration patterns (i.e. signature recognition) from data analysis of recordings can reveal structural dynamic characteristics (e.g., natural frequencies and modes), which are of paramount importance to broad-based applications in structural engineering, such as structural model validation and updating, condition assessment and monitoring, and damage diagnosis and detection.

As an alternative to signature recognition with the use of Fourier-based or wavelet data processing, this paper presents a new application of Hilbert-Huang Transform (HHT) in structural damage signature recognition from vibration records. In particular, the HHT was used to analyze controlled field vibration tests of a substructure of the Trinity River Relief (TRR) Bridge No. 4 in Texas in its intact, minor- and severe-damage states. The interpretation of the HHT analysis of the vibration data is based on the following observations, assumptions, and theories of vibration and HHT. (1) Structural vibration to a given excitation should reveal its proper frequency content, which includes driving and natural frequencies of the whole structure and/or local members, and noise frequencies. (2) When a member of the structure is damaged, its stiffness is reduced in comparison to a member without damage. Therefore, vibration recorded at the damaged member should show larger vibration amplitude at lower frequency than the vibration at a similar member without damage. (3) While the aforementioned damage and associated stiffness reduction, is large enough with respect to that of a local structural member, it might still be small in comparison with the whole structural stiffness. Consequently, vibrations recorded on the other members might not be sensitive to such a localized damage. In other words, for damaged or undamaged structure, vibrations at the member other than the to-be-damaged or damaged member will show almost the same vibration amplitude at almost the same natural frequencies. (4) Since the HHT method can identify the instantaneous frequency of measured vibration via Hilbert spectrum, the frequency of vibration on damaged member is expected to be measurably less than the frequency of sound members. This leads to the HHT identification of the damaged structural member.

The HHT analysis of the test data from the TRR bridge favorably supports the above assertion. Accordingly, an HHT-based structural health monitoring procedure is proposed.

HHT ANALYSIS OF DYNAMIC TEST DATA FOR INTACT, EXCAVATED AND BROKEN PILES

The HHT method is first briefly summarized from Huang et al. (1998). It consists of Empirical Mode Decomposition (EMD) and Hilbert Spectral Analysis (HSA). Any complicated data set can be decomposed via EMD into finite, often small, number of intrinsic mode functions (IMF) that admit a well-behaved Hilbert transform. The EMD explores temporal variation in the characteristic time scale of the data and thus is adaptive to nonlinear, nonstationary data processes. The HSA defines an instantaneous or time-dependent frequency of the data via Hilbert transformation of each IMF component. These two steps of data processing (i.e., EMD and HSA), namely HHT analysis, represent a generalized version of Fourier expansion. Mathematically, the HHT representation of data $X(t)$ is

$$X(t) = \Re \sum_{j=1}^n a_j(t) e^{i \int \omega_j(t) dt}, \quad (1)$$

where \Re denotes the real part of the value to be calculated, and both amplitude $a_j(t)$ and frequency $\omega_j(t)$ are associated with the j -th IMF component and function of time. Eq. (1) is qualitatively different from the Fourier series representation of

$$X(t) = \Re \sum_{j=1}^N A_j e^{i \Omega_j t} \quad (2)$$

where A_j is the Fourier transform of $X(t)$, a function of time-independent frequency Ω_j . Of importance, typically $n \ll N$. It should be emphasized here that the instantaneous frequency has physical meaning only through its definition on each IMF component as in Eq. (1); by contrast, the instantaneous frequency defined through the Hilbert transform of the original data is generally less directly related to frequency content (Huang et al., 1998). This special ability, together with Eqs. (1) and (2), implies that Fourier-based frequency Ω_j is essentially a special case of HHT-based instantaneous frequency $\omega_j(t)$. As the window length reduces to zero in which the data are analyzed with Fourier transformation, the Fourier-based frequency approaches the HHT-based frequency. By the Heisenberg uncertainty principle, however, the window length for Fourier analysis can never be zero. Therefore, Fourier-based frequency is dependent on window-length; it is thus locally averaged - not truly instantaneous.

The HHT method was used to analyze the data from Bent 12 of TRR bridge. Fig.1 shows the structural configuration of Bent 12 in its severe-damage state under a stationary vertical excitation in the middle of the deck. Figs. 2a and 2b show respectively the time histories of vertical excitation (or forcing function) and its corresponding vertical (or along-column) vibration response at sensor 15 (vertical seismic accelerometer – a horizontal accelerometer was also in line with the bent) with the structure in its intact state. Both time histories are highly nonstationary, with the frequency increasing almost linearly from 5 Hz at 0.5 sec to 75 Hz at 5.5 sec. The vertical excitation was also applied over the bent between each of the outside pile pairs.

Figs. 3a,b depict contour plots for the Hilbert spectra of the excitation and vibration time histories shown in Figs. 2a and 2b, i.e., the temporal-frequency energy distribution of the excitation and vibration signals. Fig. 3a shows that the excitation contains a dominant energy with the frequency increasing with time, i.e., from 5 Hz at 0.5 sec to 75 Hz at 5.5 sec. For convenience in later use, the dominant frequency content is referred to as the *dominant increasing driving frequency* or DIDF. The excitation also has energy at other frequencies such as high frequencies ranging from 20 to 45 Hz between 0.5 and 1 sec as shown in Fig. 3a, which can be verified from the chirped sine force excitation time history shown in Fig. 2a.

According to vibration theory, the frequency content of the vibration response should contain primarily both the driving frequencies depicted in Fig. 3a and the natural frequencies of the structure. This is verified by Fig. 3b. Fig. 3b shows the energy with a primary frequency content linearly increasing with time, which is the signature of excitation corresponding to the DIDF. In addition to the energy at DIDF inherent from excitation, Fig. 3b also illustrates an energy concentration in the frequency range of 10 to 20 Hz (others from 20-75 Hz) at times of

between one and two seconds. This phenomenon can be regarded as the energy contributed from the structural vibration modes at a couple of lower (higher) natural frequencies, or the signature of the structure. These vibration modes are likely excited by the excitation at 0.5-1 sec with a low-frequency content of 5-15 Hz that is close to the fundamental natural frequency of the structure. As time goes on (say 2-3 sec), the vibration at those frequencies dies down quickly due to damping, or is too small to be shown in the figure in comparison with strong DIDF energy.

Since the modal vibration results showed that the fundamental natural frequencies of the structure should be measured from the vibration during 1-2 sec, all the following figures of the Hilbert spectra are presented with time less than 3 sec and frequency less than 40 Hz.

Fig. 4a enlarges the Hilbert spectrum of vibration response at sensor 15 with the structure in its intact state. Except the DIDF, we believe that all the other energy concentration shown in Fig. 4a is attributed primarily by the structure itself. We now focus on the energy at frequency up to 15 Hz during 1-2 sec. The energy below roughly 10 Hz is much less than that above 10 Hz. This response energy is believed to be generated by the excitation at the DIDF during 0.5-1 sec and the driving frequency of 6-15 Hz at around 1+ sec in Fig. 3a. If the fundamental natural frequency falls in the driving frequency range of 5-15, the response energy at the fundamental natural frequency should be much stronger than that at frequency lower, but not necessarily stronger than that at frequency higher since there exist second and higher natural frequencies. Fig. 4a suggests that the fundamental natural frequency is likely around 10 Hz, slightly lower than what the Fourier spectral analysis of the data predicts (i.e., 15 Hz from Sanayei and Santini, 1998). Note that Fourier spectral analysis typically supplies distorted, indirect or incomplete information on the nature of the nonlinear, nonstationary data (e.g., Huang et al., 1998).

Fig. 4b shows the Hilbert spectrum of vibration response at sensor 15 with the structure in its minor-damage state. Besides the applied DIDF, the vibration energy concentration during 1-2 sec has lowered its frequency to 7 Hz at about 1.4 sec. The observed 7 Hz in the minor-damage state could be related to the mixed natural frequency of the pile and bent, since the vibration at sensor 15 should reflect the dynamic characteristics of both the whole structure and the local member. The excavated soil, i.e., the structure in the minor-damage state, reduces the stiffness of the pile and thus the fundamental natural frequency of the bridge pier. This is the signature of local damage in the recordings.

Such an explanation can be further strengthened by Fig. 4c, which shows the Hilbert spectrum of vibration response at sensor 15 with the structure in its severe-damage state. As seen in the figure, the dominant frequency has decreased to 3 Hz at 1.7 sec. It should be pointed out that the above explanation is simply based on the observation with the aid of vibration theory without proof. While further model-based validation is the subject of a continuing study, a very simple, rough estimation of whether the above observation is conceivable is presented in Table I below.

Since accelerometer sensor 15 is mounted on the column with one end connected to the beam and the pile end buried in the soil, the dominant vibration recorded should more likely contain the dynamic features of the column itself. To examine the change of fundamental natural frequency of the column at three damage states, we can roughly model the column with different boundary conditions and lengths. In particular, the boundary conditions are approximated as

fixed-fixed with length 7' for column in the intact state, fixed-fixed with length 16' in the minor-damage state, and fixed-free with length 7' in the severe damage. The above simple boundaries were chosen not only because they very rudely model the real vibration of the column but also because they have simple, exact solutions for the fundamental natural frequency. This simple theoretical model shows that the relative change of the fundamental natural frequency in the minor- and severe-damage states with respect to that in the intact state is 56% and 68%, respectively. In contrast, the pertinent relative change with the use of the observed fundamental natural frequency is 50% and 70%. The detailed comparison can be seen in Table 1. The observed results are very close to the theoretical ones. While this comparison suggests that the previous explanation might be permissible, it nevertheless indicates that the explanation is likely correct. Further solid validation is still needed both experimentally and theoretically of the HHT method in this regard.

The HHT analysis of vibration at sensor 15 with the Bent in three states shows that the HHT method might clearly recognize the signature difference of sequential damage in a structural member in terms of natural frequency from recordings. As a comparison, we now present the HHT analysis of corresponding vibration at sensor 13, which is removed from the damage location. Figs. 5a-c present the Hilbert spectra of vibration data at sensor 13 for the structure in its intact, minor- and severe-damage states respectively. All the figures show that the lowest dominant frequency of structural vibration is around 10 Hz in 1-2 sec. This not only confirms that the fundamental natural frequency of the whole structure and its members can likely be distinguished from the driving frequency by the HHT analysis, it also suggests that HHT analysis is sensitive to the change in vibration characteristics due to local damage.

MODAL VIBRATION TESTING AND ANALYSIS RESULTS

Modal testing and analysis was also conducted of Bent 12 in its intact, minor-damage (excavated) and severe-damage (excavated and broken pile) states during the research. Flexibility transfer functions (displacement/force) are the inverse of stiffness and were calculated for various vertical accelerometer nodes. In order to quickly examine the relative changes, A photograph of the Vibroseis over a bridge bent from the field testing is shown in Figure 6. Figure 7 shows the flexibility transfer function results in inches/pound force (in/lbf) versus frequency for the intact, excavated and broken pile (no pile) states for Node 10 which is about 3 ft higher than nodes 13 and 15 and located on the pile between the sound pile and the broken pile in Figure 1. Review of Figure 6 shows that the intact case was the least flexible (stiffest) and the excavated and broken pile case was the most flexible (least stiff). Further examination of this figure shows a slight shift in frequency of the peak responses downward with damage, but no dramatic change. Curve-fitting of the data to extract vibration mode shapes, frequencies and damping added little to the identification of intact, minor- and severe-damage states. However, the results of the flexibility modal test results (which are in a sense a dynamic load test) did show up to 50% differences in flexibility/stiffness between the intact and severe-damage states. Thus, if testing was done prior to an earthquake or other catastrophic event and after such an event, one could determine the loss of foundation stiffness with modal tests and analyses of the flexibility transfer functions. The lack of greater sensitivity on the frequency shift is attributed to the averaging effects of Fast Fourier Transforms over the full measurement time window. The HHT approach provides an instantaneous FFT in a sense at each instant in time that identifies the brief

moments when the lower-frequency response associated with non-linear effects due to reduced stiffness due to damage occur in the modal vibration data.

STRUCTURAL MODELING AND PARAMETER ESTIMATION RESULTS

The structural parameter estimation approach was unable to find a consistent, correct solution to the intact versus excavated versus broken pile cases (Sanayei et al, 1998). It may be that the fundamental problem is that the effects of the foundation damage are too small for parameter estimation and buried in the overall modal vibration response of the structure.

PROPOSED STRUCTURAL HEALTH MONITORING

The above experimental study presents the HHT analysis results from vibration tests of bridge substructures in their intact, minor- and severe-damage states. It reveals that the HHT-based signature recognition is likely able to identify the local dynamic properties. In addition, comparison of the HHT analysis of two recordings from damaged and sound structural elements in one condition state of the structure can tell the damage signature difference of local structural members. This eliminates the need of a priori data required in traditional damage diagnosis, and thus significantly improves the efficiency in data collection. Based on the study, a novel signature-recognition technique for structural health monitoring and damage detection is proposed as follows.

- (1) Two or more similar structural members (e.g., two of four columns in a bridge with the same size, cross-section, and materials) are selected for a non-destructive vibration test, each of which has one sensor mounted (e.g., accelerometer). The test is subjected to a dynamic excitation acting at a location close to, but not directly on the members. A computer data acquisition system will digitize and store the sensor output to the excitation. This will result in two sets of data.
- (2) In the HHT method, the two data sets are first decomposed into a number of intrinsic mode function (IMF) components in the empirical mode decomposition (EMD) process, each of which is then input to the Hilbert spectral analysis (HSA) to compute the Hilbert spectrum. Consequently, the driving frequency, natural frequency, and other frequency contents can be identified partially, if not completely, by analyzing the Hilbert spectra and IMF components. The time data should also be analyzed with spectral/modal methods to determine the resonant, natural frequencies as well.
- (3) If the HHT determined natural frequencies of the two members are different, the member with the lower frequency has damage while the other is health, or former has more severe damage than the latter. On the other hand, if the frequencies are the same, both members are either undamaged or damaged to the same degree. In that case, the testing will be repeated with a third member involved, or a priori data from testing the same structure is needed as a reference.
- (4) After identifying the damaged member, one can apply the excitation at different locations in the damaged member and record a series of vibration data sets at one sensor location.

- (5) Analyze the above data sets using step 2.
- (6) If one of the above data set shows the lowest natural frequency of the member, the location of the pertinent excitation is exactly or close enough to the damaged spot.

The reasons for the last three steps are provided as follows. When the excitation is acting directly on the damaged location, the impact to the structure at that location will be the strongest. Even if the load is within the design range, the damaged member should have nonlinear responses, i.e., the response should have lower natural frequencies at certain time period. On the other hand, the vibration responses of the structure should remain elastic and linear if the excitation acts neither directly nor closely enough to the damage spot. Since the HHT is able to identify the instantaneous frequency of data, the damaged member can be found by identifying the lowest natural frequency of vibration from the series of data sets.

CONCLUSIONS

This FHWA sponsored study (Olson, 2003) shows the HHT analysis results of modal vibration test data of bridge structures in their intact, minor- and severe-damage states. It reveals the following.

- (1) The HHT method in structural damage diagnosis is found to be effective and sensitive for signature recognition of at least one type of structural damage (e.g., the one used in the study). While such an observation relies upon further validation, the HHT approach to the non-destructive vibration data presented in the study should be useful for structural studies.
- (2) According to the HHT analysis of the destructive vibration testing data, an HHT-based structural damage diagnosis is proposed. If the effectiveness of the proposed diagnosis is verified, it has at least two unique features different from traditional methods:
 - (a) It needs only a few sensors (minimum of two recommended for substructures) and possibly no a priori data from undamaged structure, which makes data collection simple and cost-effective.
 - (b) It uses the HHT method to analyze the above measured data to reveal the change of temporal-frequency energy of various intrinsic oscillation modes that are extracted from the data. This enables the diagnosis to be sensitive to local member damage that is associated with certain intrinsic modes.

REFERENCES

1. Huang, N.E., S. Zheng, S.R. Long, M.C. Wu, H.H. Shih, Q. Zheng, N-C. Yen, C.C. Tung, and M.H. Liu, "The Empirical Mode Decomposition And Hilbert Spectrum For Nonlinear And Nonstationary Time Series Analysis." *Proc. Roy. Soc Lond., A* 454 903-995 (1998).

2. Sanayei, M. and E.M. Santini, "Dynamic bridge substructure evaluation and monitoring system," *Tufts University Report from FHWA Grant to Olson Engineering, Inc. (1998)*.
3. Olson, L. D., *Final US Department of Transportation Federal Highway Administration (FHWA) Project Report for Contract No. DTFH61-96-C-00030 (2003)*.

	Boundary condition with length	Theoretical frequency (F)	Observed frequencies (f)	Relative change of frequency with respect to frequency at intact state	
Intact	Fixed-fixed with $l=7'$	$F_i = \frac{1}{2l} \sqrt{\frac{E}{\rho}}$	$f_i = 10$ Hz	N/A	
Minor-damage	Fixed-fixed with $l=16'$	$F_m = \frac{1}{2l} \sqrt{\frac{E}{\rho}}$	$f_m = 5$ Hz	$(F_i - F_m)/F_i = \mathbf{56\%}$	$(f_i - f_m)/f_i = \mathbf{50\%}$
Severe-damage	Fixed-free with $l=11'$	$F_s = \frac{1}{4l} \sqrt{\frac{E}{\rho}}$	$f_s = 3$ Hz	$(F_i - F_s)/F_i = \mathbf{68\%}$	$(f_i - f_s)/f_i = \mathbf{70\%}$

Table 1: Fundamental natural frequencies of a column in three states by simple theoretical models and their comparison with observation from HHT analysis of destructive testing data.

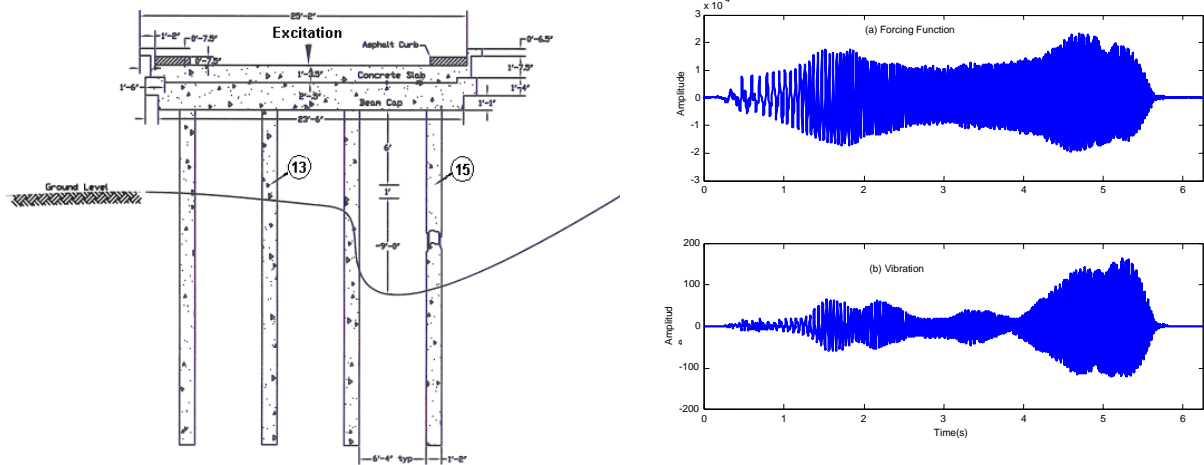


Figure 1 (left): Vibration tests of Bent 12 in the Trinity Relief River Bridge No. 4 under excitations at the middle of the deck. The three states of the bridge are: (1) **Intact state**: the column with accelerometer sensor 15 (the rightmost column) was not broken and soil around the column had the same height as the soil around the column with sensor 13 (second to the most left column), (2) **Minor-damage state**: the column with sensor 15 was not broken, but soil around the column was excavated, and (3) **Severe-damage state**: the column with sensor 15 was broken with the steel bars left only and soil around the column was excavated.

Figure 2 (right): Bridge in intact state. (a, top) Forcing function and (b, bottom) Recorded vibration at sensor 15.

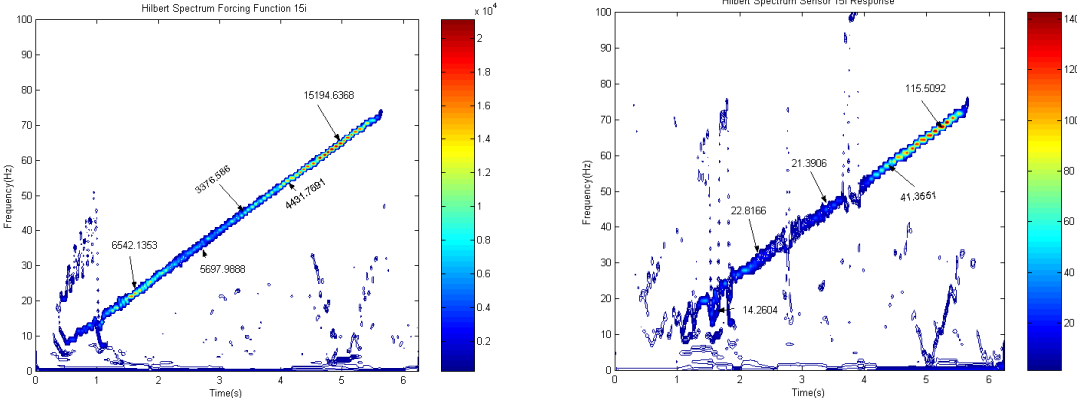


Figure 3a (left): Hilbert spectra of forcing function for vibration at sensor 15 in intact bridge.

Figure 3b (right): Hilbert spectra of vibration at sensor 15 in intact bridge.

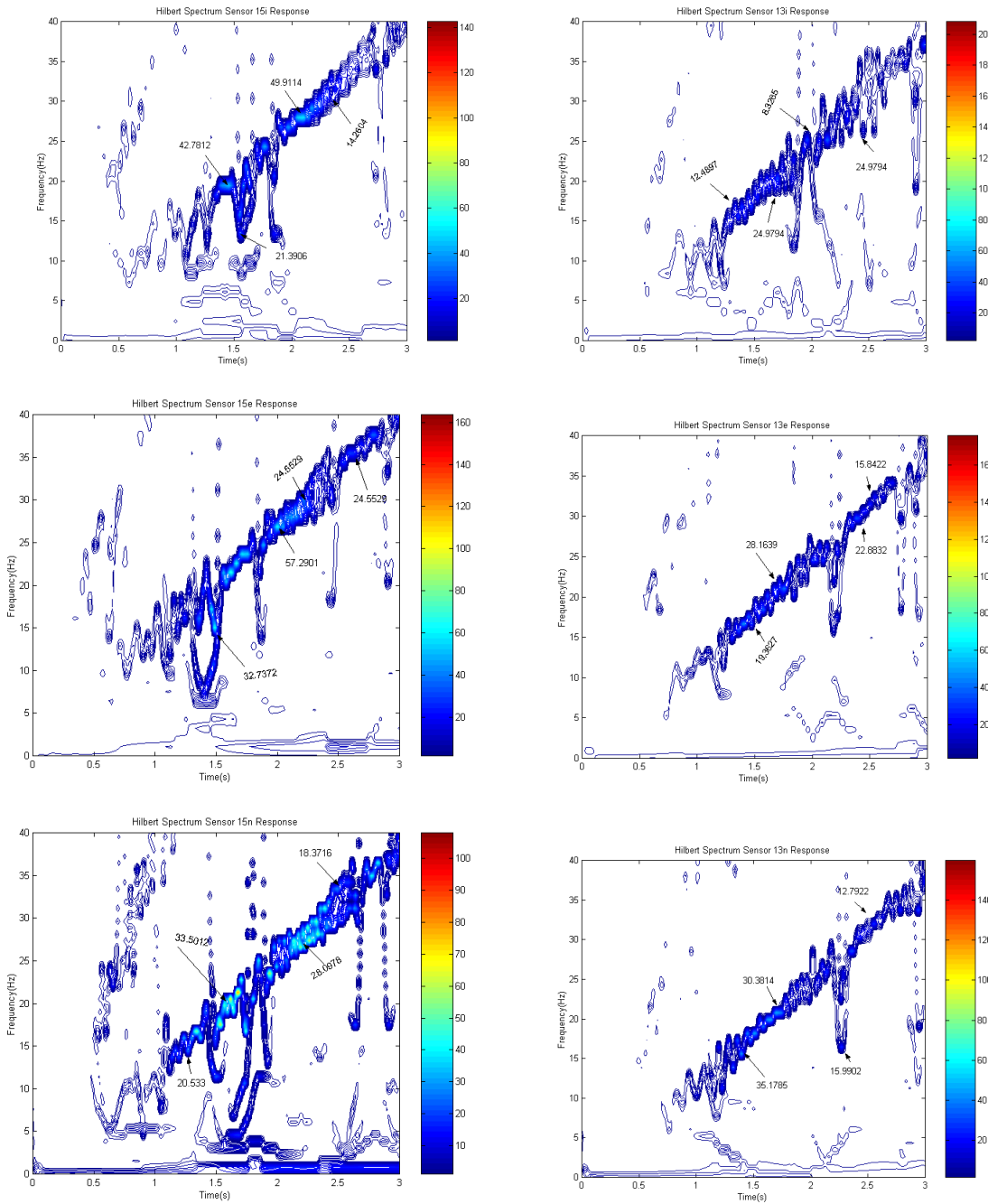


Figure 4 (left): Hilbert spectra of vibration at sensor 15 of the bridge in its intact state (a, top), minor-damage state (b, middle) and severe-damage state (c, bottom).

Figure 5 (right): Hilbert spectra of vibration at sensor 13 of the bridge in its intact state (a, top), minor-damage state (b, middle) and severe-damage state (c, bottom).



Figure 6: Vibroseis over Pile Bent on Trinity River Relief Bridge No. 4

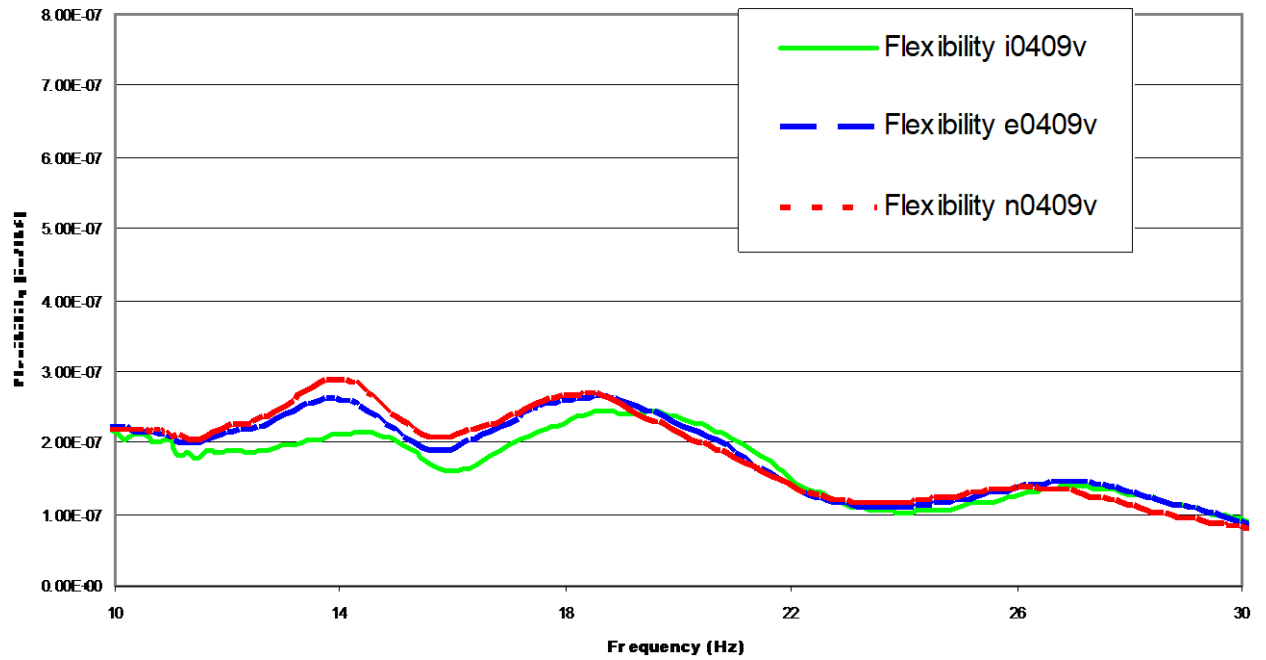


Figure 7: Comparison of Modal Vibration Test Result Flexibility Transfer Functions for Node 10 (3 ft higher than Nodes 13 and 15 in Figure 1 and on the Pile between Nodes 13 and 15) in intact (bottom plot), minor-damage (excavated piles) and severe-damage (broken pile below Node 15) states.